Applied Thermal Engineering 147 (2019) 113–121

Contents lists available at ScienceDirect

Applied Thermal Engineering

journal homepage: www.elsevier.com/locate/apthermeng

Research Paper

# Falling film evaporation and nucleate pool boiling heat transfer of R134a on the same enhanced tube

Wen-Tao Ji[a,*], Er-Tao Zhao[a], Chuang-Yao Zhao[a], Hu Zhang[b], Wen-Quan Tao[a]

[a] Key Laboratory of Thermo-Fluid Science and Engineering of MOE, Xi'an Jiaotong University, Xi'an 10049, China
[b] State Key Laboratory for Strength and Vibration of Mechanical Structures, Xi'an Jiaotong University, Xi'an 710049, China

## HIGHLIGHTS

- Falling film evaporation heat transfer coefficients was augmented by a factor of 2.1–4.9.
- The pool boiling yielded a higher heat transfer coefficient at higher heat flux for enhanced tube.
- Pool boiling and falling film evaporation were both dominated by the phase change heat transfer.

## ARTICLE INFO

*Keywords:*
Falling film evaporation
Heat transfer
Refrigerant
Tube bundle

## ABSTRACT

Falling film evaporation and pool boiling of R134a outside a typical reentrant enhanced tube was investigated with an experimental approach. Experimental data from literature with other refrigerants were also compared. The saturation temperature was 11 °C. It was found that the overall heat transfer coefficient for the enhanced tube was as much as 3 times higher than smooth tube. Shell-side falling film evaporation heat transfer coefficient increased by a factor of 2.1–4.9. Pool boiling yielded a higher heat transfer coefficient at higher heat flux for the same enhanced tube. The dependence of falling film evaporation heat transfer coefficient on the heat flux was also different from pool boiling for the same tube. Although the bubbles in pool boiling were pushed up by buoyancy and in falling film evaporating were driven by the flow of films, the transmission of energy were both dominated by the phase change heat transfer. The contribution of forced convection to falling film evaporation heat transfer coefficient is weak compared with phase change heat transfer.

## 1. Introduction

Falling film evaporation is one of the most efficient heat transfer methods. It has a number of advantages over the flooded mode in air-conditioning systems. The shell-side of falling film evaporator need not to be filled with large quantities of liquid refrigerant, and only thin film is required to cover the tube surfaces sufficiently. This can be cost competitive for the chiller manufactures. In recent years, HCFC and HFC phase-out also began to motivate widely application of falling-film evaporators. Falling film evaporation as a promising alternative might finally replace flooded evaporators in the future if new hydro-fluoroolefin (HFO) refrigerants with low global warming potential (GWP) are widely used in the chillers with large capacity. It also shows improved heat transfer performance over the flooded evaporators, especially in the heat flux lower than 20 kW/m$^2$. Besides, improved lubricant recovery and reducing risks associated with refrigerant leakage are also the superiorities of falling film evaporators.

Despite having many advantages, a lot of challenges still exist, such as complexity of the system and lack of understanding on falling film evaporating [1–3]. Tube layout, pitches, vapor flow, and surface geometry are also the major influencing factors [4–6] for large capacity chillers. The configuration and design of falling film evaporators are the major concerns for large-scale applications. Liquid film spray rate should change as the changes of heat load. An uneven distribution of film over the tubes has severe impact on the heat transfer. It should involve a continuous upgrading of the design. Parameter optimization and systematically comparison on the falling film evaporation and pool boiling should be rather important. The following is a brief review on the investigations for both pool boiling and falling film evaporation of refrigerants outside different enhanced tubes.

Falling film evaporation of ammonia onto the horizontal smooth-tube bundle was tested by Zeng et al. [7,8]. The effects of heat flux, saturation temperature, spray flow rate, nozzle height, and nozzle type were investigated. It was speculated that the amount of refrigerant

* Corresponding author.
*E-mail address:* wentaoji@xjtu.edu.cn (W.-T. Ji).

https://doi.org/10.1016/j.applthermaleng.2018.10.062
Received 10 June 2018; Received in revised form 23 September 2018; Accepted 15 October 2018
Available online 17 October 2018
1359-4311/ 

**Nomenclature**

*List of symbols*

| | |
|---|---|
| $A$ | area, $m^2$ |
| $c_i$ | enhanced ratio of tube side heat transfer coefficient |
| $c_p$ | specific heat, $J \cdot kg^{-1} \cdot K^{-1}$ |
| $C$ | coefficient of Cooper equation |
| $d$ | diameter of tube, mm |
| $e$ | height of outside fin, mm |
| $f$ | friction factor |
| $h$ | heat transfer coefficients, $W \cdot m^{-2} \cdot K^{-1}$ |
| $H$ | height of inside fin, mm |
| $k$ | overall heat transfer coefficients, $W \cdot m^{-2} \cdot K^{-1}$ |
| $L$ | tube's tested length, m |
| $\dot{m}$ | mass flow rate, $kg \cdot s^{-1}$ |
| $m$ | coefficient in Cooper equation |
| $M$ | molecular weight of refrigerant |
| $P_r$ | reduced pressure in Cooper's equation |
| $q$ | heat flux, $W \cdot m^{-2}$ |
| $Re$ | falling film Reynolds number |
| $R_p$ | average surface roughness of plain tube, μm |
| $R_w$ | thermal resistance of tube wall |
| $t$ | external fin thickness,mm |
| $T$ | temperature, °C |
| $u$ | velocity, m/s |

*Greek alphabet*

| | |
|---|---|
| $\Phi$ | heat transfer rate, W |
| $\lambda$ | thermal conductivity, $W \cdot m^{-1} \cdot K^{-1}$ |
| $\Gamma$ | falling film flow rate on one side of tube per unit length, $kg \cdot m^{-1} \cdot s^{-1}$ |
| $\Delta T_m$ | logarithmic mean temperature difference |
| $\Delta p$ | pressure drop, Pa |
| $\eta$ | dynamic viscosity, $N \cdot s \cdot m^2$ |

*Subscript*

| | |
|---|---|
| c | cooling |
| e | evaporating |
| i | inside of tube |
| in | inlet of tube |
| m | number of tubes fixed in the evaporator |
| n | number of tubes fixed in the condenser |
| o | outside of tube |
| out | outlet of tube |
| p | pump |
| r | refrigerant |
| s | saturation |
| w | wall |

retained in the tube bundle under falling film evaporation was comparable to that in pool boiling. The reduction in the refrigerant charge for the falling film evaporator might be chiefly in the volume between the bundle and the vessel wall. It was found that the falling film evaporation heat transfer coefficient primarily increases with heat flux and saturation temperature. Compared with the pool boiling heat transfer at the same experimental conditions, the falling film evaporation heat transfer coefficient can be up to 65% or higher.

Falling film evaporation and pool boiling of R134a and R236fa outside a single tube and tube bundles were investigated by Christians and Thome [9,10]. Two enhanced boiling tubes, the Wolverine Turbo-B5 and Wieland Gewa-B5, were tested. The film Reynolds numbers was from 0 to 3000, and heat flux was between 15 and 90 $kW/m^2$. It was found that the heat transfer coefficient all decreased with increasing heat flux in pool boiling. Falling film evaporating heat transfer was basically not dependent on heat flux. The heat transfer coefficient in falling film evaporating was much higher, especially for tube Turbo-B5. At heat flux of 40 $kW/m^2$ and higher film Reynolds number, the falling film heat transfer coefficient was in the range of 30–40 $kW/m^2K$ for both refrigerants. In falling film evaporation, compared with single array tests, the bundle effect was not obvious for different layouts.

Falling film heat transfer outside Turbo-B5 and Gewa-B5 tubes were also investigated by Rooyen and Thome [11] with R-134a and R-236fa. It showed Turbo-B5 tube had a fairly constant heat transfer coefficient around 30 $kW/m^2K$ for R134a and 23 $kW/m^2K$ for R236fa in the test heat flux. However, Gewa-B5 tube had a dependence on heat flux for both fluids. The heat transfer coefficient was higher at lower heat flux and decreased from the peak of 35 $kW/m^2K$. The Gewa-B5 had a more consistent heat transfer coefficient with R-236fa around 20 $kW/m^2K$. Identification and prediction the onset of dry-out in the tube bundle were also studied [11]. According to the investigation, falling film heat transfer performance was equal or higher than pool boiling.

Falling film evaporation of R134a and R123 outside four enhanced tubes were investigated by Zhao et al. [6] recently. It was found that the heat transfer coefficient of R134a can be 2–3 times higher than R123 at the film flow rate larger than 0.025 kg/m.s. For R134a, two of the four enhanced tubes provided higher heat transfer coefficients. However, it was found to be opposite in the experiment with R123. It could be

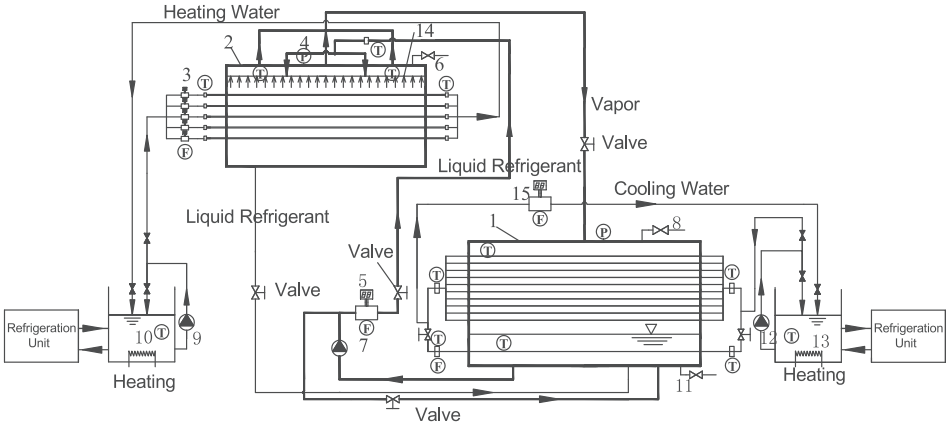


**Fig. 1.** Schematic diagram of experimental apparatus.

related to the thermal properties of refrigerants and surface structures. The vapor flow effect across tube bundle were also investigated by Ji and Zhao et al. [5,12]. Extra vapor velocity at the smallest clearance in the tube bundle varied from 0 to 3.1 m/s. For the upward vapor flow, both positive and negative effects were observed as the increment of vapor velocity. Positive effects were predominant for the two tubes in the top positions and higher vapor velocity. For the cross vapor flow, with the increase of vapor velocity, the heat transfer coefficients showed the general trend of first increase then decrease. The cross vapor generally had a notable enhancement effects on heat transfer at larger film flow rate or at the lower heat flux.

There are also a lot of investigations on the heat transfer performance of pool boiling outside the horizontal tubes. It includes the investigations on the low GWP refrigerants [13] and different types of enhanced tubes [14–16].

As indicated above, falling film evaporators had the potential to replace flooded evaporators in the refrigeration industry due to many advantages. Although it is supposed that the heat transfer coefficient of falling film evaporation is higher than pool boiling [17], it is still in doubt due to many influencing factors for the process. In order to have a full or clearer understanding on the mechanisms of falling film evaporation, a comprehensive investigation on the comparison between pool boiling and falling film evaporation outside one enhanced tube was conducted in the present investigation.

In the following sections, after an introduction on the experimental setup, test procedure and data reduction method, the test results are presented. The last section is some conclusions.

## 2. Experimental apparatus

The experimental apparatus includes three loops: refrigerant, heating and cooling water circulating system. Fig. 1 schematically depicts the test apparatus and the three loops.

The refrigeration circulation loop is made of stainless steel. It consists of the following components: evaporator, condenser, canned motor pump, mass flow meter and film distributor. Liquid refrigerant is charged and stored in the condenser, then pumped to the evaporator through the canned motor pump. Pressurized liquid refrigerant enters the evaporator and distributed uniformly outside the horizontal tested tube bundles. Then liquid film evaporates outside the horizontal tube bundles and changes into vapor. Liquid refrigerant that doesn't evaporate will return to the refrigerant storage tank from the bottom of evaporator by gravity. The vapor flows to the condenser from the top of evaporator and condenses from its gaseous to liquid state outside the tube bundle mounted in the condenser. This is the circulation of refrigerant. The liquid refrigerant flow rate is measured with Coriolis mass flow meter (The error is within ± 0.1% in the entire measurement range). The whole apparatus is enwrapped with rubber plastic of thickness 60 mm for insulation.

In order to obtain a uniform liquid distribution along the test tubes, the liquid film distributor consists of two stage of distributing process (See Fig. 2). Liquid refrigerant enters pre-distributer with two entrances. When the liquid film leave the bottom of pre-distributor it reaches the second stage distributor. The second stage is a stainless rectangular box with small holes in the bottom. The distributing box opens to the evaporator and the film leaves the box by gravity.

The tube bundles are fixed in the evaporator with single row. Test section in the evaporator and condenser has a length of 2039 mm. The test tubes have the diameter of 25.4 mm and the longitudinal tube pitch is 31 mm. The temperature of water and refrigerant is monitored with PT100 transducers with an accuracy of ± 0.05 °C. The internal diameter of evaporator and condenser are both 450 mm. The evaporator and condenser both have the glass windows with internal diameter of 80 mm. It can be used to monitor and observe the film flow outside the tube bundles.

If the tested tube is fixed in the bottom of condenser and submerged in the liquid refrigerant, pool boiling experiment is conducted. Then the refrigerant boils outside the single test tube, converts to vapor and condenses outside the condensing tubes fixed in the top of condensers. This is the circulation of refrigerant for pool boiling. The pool boiling and falling film experiments were performed separately.

Heating and cooling water provide water for the evaporator and condenser. Heating water flows through the inside of test tubes in falling film evaporation or pool boiling, and returns to the hot water tank. Cooling water flows through the condensing tubes fixed in the condenser. The heating and cooling water tanks are the thermostatic water baths. The heating and cooling water tank both have the refrigeration and electric heating systems. The volumes of two tanks are both 3 $m^3$. The temperatures of water flow rate are also measured by PT100 transducers with an accuracy of ± 0.05 °C. A digital voltmeter having the resolution of 100 μΩ is used to measure the electric resistance of temperature transducers. Flow rates are measured by electromagnetic flow meters (accuracy is within 0.1% in the whole measurement range). The pressure was measured by a pressure gauge which has the accuracy within ± 0.05% of full scale (0–2 MPa). The accuracy of differential pressure transmitter is within 0.1% of full scale (0–62.16 kPa).

The cross section and micrographs of the test tubes are shown in Fig. 3. The specifications are given in Table 1, where $d_i$ and $d_o$ are the diameters of embryo tube. The enhanced tube is a typical reentrant cavity tube with overlapped tunnels under the surface specially designed for pool boiling.

## 3. Experimental procedure

High-pressure nitrogen up to 1.2 MPa was charged into the refrigerants circulation system to check the tightness. After all the leaks were eliminated, the pressure of 1.2 MPa was kept at least for 24 h, and the high pressure nitrogen was discharged. Then, the system was evacuated by a mechanical vacuum pump to an absolute pressure of at least 1000 Pa. Keep the vacuum for at least 5 h, if no leak was detected, then the refrigerant R134a was charged into the system through the valves installed on the top of condenser.

Furthermore, the system was charged with refrigerant. A small amount of liquid refrigerant was firstly charged into the system, then evacuates with a vacuum pump. Repeat the process for at least four times until the non condensable gases in the system was reduced to a minimum amount. Finally, the refrigerant was charged into the liquid refrigerant storage tank. The height of liquid level was at least 50 mm over the top of boiling tubes in the condenser.

In the experiment, the deviation of saturation temperature measured by temperature sensor and that corresponding to pressure should be within 0.1 °C. If the deviation of the two temperatures exceeded, the vapor refrigerant was exhausted by the valves fixed in two ends of

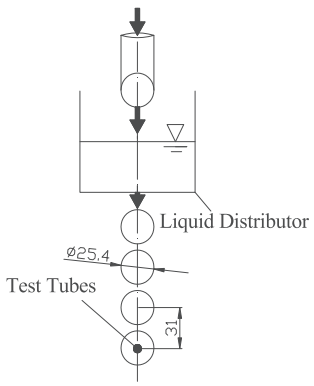


**Fig. 2.** Schematic diagram of test tubes and falling film distributor (all dimensions are in mm).

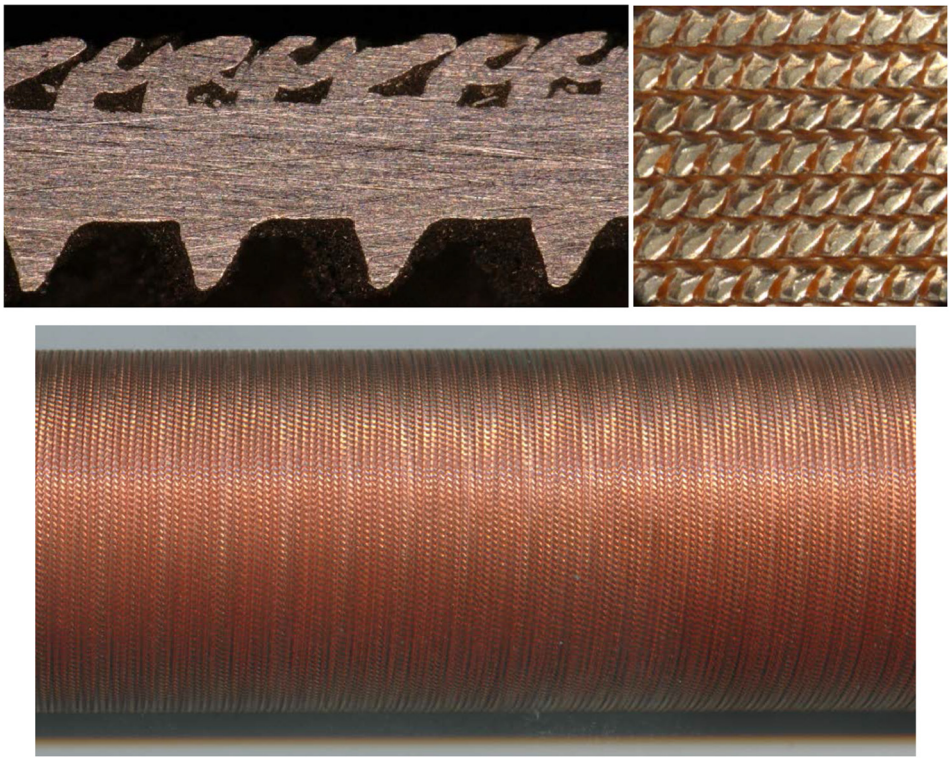

**Fig. 3.** Cross sections of enhanced tube.

condenser and evaporator to meet this requirement.

The experimental apparatus was running at least 1 h every day before the data acquisition until the experimental system reached a steady state. The steady state was characterized by (1) the variation of required saturation temperature of refrigerant was in the allowed range, usually ± 0.1 K and (2) the fluctuation of water temperature at inlet and outlet of condenser and evaporator was all within ± 0.1 K.

## 4. Data reduction and uncertainty analysis

The overall, tube and shell side heat transfer coefficient were obtained with the following equations.

Heat duty of water in falling film evaporation or pool boiling:

$$\phi_{e,m} = \dot{m}_{e,m} c_{p,m} (T_{e,m,\mathrm{in}} - T_{e,m,out}) \tag{1}$$

Cooling power of cooling water:

$$\phi_c = \dot{m}_c c_p (T_{c,out} - T_{c,in}) \tag{2}$$

In the two equations above, $T_{\mathrm{e,m,in}}$, $T_{\mathrm{e,m,out}}$ are the inlet and outlet temperatures (K) of heating water for the $m_{\mathrm{th}}$ tubes, respectively. $T_{\mathrm{c,in}}$, $T_{\mathrm{c,out}}$ are the inlet and outlet temperatures (K) of cooling water. $T_{\mathrm{e,m,in}} - T_{\mathrm{e,m,out}}$ is normally in the range of 0.8–2 °C and $T_{\mathrm{c,in}} - T_{\mathrm{c,out}}$ is 1.5–2.7 °C. $c_{\mathrm{p}}$ is the specific heat capacity (J/kg.K) of heating or cooling water, corresponding to the mean temperature of inlet and outlet water. $\dot{m}_{e,m}$ and $\dot{m}_c$ are the mass flow rates (kg/s) of heating and cooling water, respectively. $m$ is the number of test tubes in falling film evaporation fixed in the evaporator. If the pool boiling experiment is conducted, only one tube is tested. The heat balance was within 3% for all the experiment. The error of heating water and cooling water should be within 0.61% and 0.95%. We analyze the uncertainty of $k$ from $\phi_{e,m}$.

Overall heat transfer coefficient of each test tube is determined with the following equation:

$$k = \frac{\phi_{e,m}}{A_o \Delta T_{m,m}} \tag{3}$$

where,

$$A_o = \pi d_o L \tag{4}$$

$\Delta T_{m,m}$is the log-mean temperature difference of each test tube in experiment:

$$\Delta T_{m,m} = \frac{T_{w,m,in} - T_{w,m,out}}{\ln\left(\frac{T_s - T_{w,m,\mathrm{out}}}{T_s - T_{w,m,\mathrm{in}}}\right)} \tag{5}$$

$T_{\mathrm{s}}$ in the equation is the saturation temperature which is obtained from the measured pressure in the evaporator according to the thermodynamics table. The shell side falling film evaporating or pool boiling heat transfer coefficient $h_{\mathrm{o}}$ is obtained with thermal resistance separation method:

$$\frac{1}{h_o} = \frac{1}{k} - \frac{A_o}{A_i}\frac{1}{h_i} - R_w \tag{6}$$

$A_{\mathrm{i}}$ is the heat transfer area of internal tube. $R_{\mathrm{w}} = \frac{do}{2\lambda_{\mathrm{w}}} \ln \frac{do}{di}$ is the thermal resistance of tube wall. $h_{\mathrm{i}}$ is the water side forced convection

**Table 1**
Specifications of tested tubes.

| Tubes | Outside diameter $d_{\mathrm{o}}$ (mm) | Inside diameter $d_{\mathrm{i}}$ (mm) | Height of outside Fin $e$ (mm) | Outside fin numbers per inch | External fin root thickness $t$ (mm) | Helix angle of internal fins (°) | Height of inside fin $H$ (mm) | Length of test section $L$ (mm) |
|---|---|---|---|---|---|---|---|---|
| Smooth | 19.06 | 16.26 | – | – | – | – | – | 2039 |
| Enhanced | 25.40 | 22.98 | 0.432 | 48 | 0.262 | 55 | 0.410 | 2039 |

heat transfer coefficients. When the inside of test tube is smooth, $h_i$ is determined by the Gnielinski equation [18]:

$$h_{ip} = \frac{\lambda}{d_i}\frac{(f/8)(\mathrm{Re}-1000)\,\mathrm{Pr}}{1+12.7(f/8)^{1/2}(\mathrm{Pr}^{2/3}-1)}\left[1+\left(\frac{d_i}{L}\right)^{2/3}\right]\left(\frac{\mathrm{Pr}}{\mathrm{Pr}_w}\right)^{0.11}$$

$$(\mathrm{Re} = 2300 - 10^6,\ \mathrm{Pr} = 0.6 - 10^5) \tag{7}$$

If the tube side is enhanced with integral-fins [19–21], the internal heat transfer coefficient $h_i$ can be written as $c_i h_{ip}$. Wilson plot is used to obtain the heat transfer enhancement ratio of internal finned tube over smooth one, $c_i$ [22]. Keep $h_o$ generally invariable during the test. That is, the saturate temperature of refrigerant and the heat flux were kept constant. Then Eq. (6) is changed into:

$$\frac{1}{k} = a\frac{1}{h_{ip}} + b \tag{8}$$

where:

$$a = \frac{d_o}{d_i}\frac{1}{c_i} \tag{9}$$

$$b = \frac{1}{h_o} + R_w \tag{10}$$

In the experiment, a group of data is taken by changing the in-tube water velocity. By the linear regression, the slope $a$ and the constant $b$ of the fitted line are obtained. Then, the enhancement ratio, $c_i$, of inner enhanced tube is determined.

Fig. 4 is the Wilson plot of smooth and enhanced tubes. The internal water velocity is from 0.8 to 3.0 m/s. The heat flux is kept invariant at 30 kW/m$^2$. Compared with Gnielinski equation, the enhanced ratios of smooth and enhanced tube are 0.99 ± 0.10 and 3.22 ± 0.10, respectively.

The falling film Reynolds number is determined with the following equation:

$$\mathrm{Re} = 4\Gamma/\eta \tag{11}$$

where $\Gamma$ is the falling film flow rate on one side of the tube per unit length (kg/m·s). It can be obtained through the Coriolis mass flow meter. $\eta$ is the dynamic viscosity (N·s/m$^2$) of refrigerant corresponding to the saturation temperature.

The friction factor is determined using the following equation:

$$f = -\frac{\Delta p d_i}{L\cdot\rho u^2/2} \tag{12}$$

where $\Delta p$ is the pressure drop in the test section, which is tested by the differential pressure transmitter. $L$ is the length of test section.

Uncertainty analysis is performed according to Refs. [23,24]. The confidence level for all measurements is 95%. The estimated uncertainties of $k$ are less than 3.6%. The uncertainty of $h_o$ is estimated using the method suggested in Refs. [25,26]. If the uncertainty of Gnielinski equation [18] is regarded as ± 10%, the maximum uncertainty of the falling film evaporation and pool boiling heat transfer coefficient, $h_o$, is estimated to be less than 13.7% for all the measurements.

## 5. Results and discussion

### 5.1. Validation of the experimental system

In order to check the reliability of experimental system, experimental results on smooth tube were compared with Cooper's equation [27,28] in pool boiling.

$$\text{Cooper's equation: } h_o = Cq^{0.67}M_r^{0.5}P_r^m(-\log P_r)^{-0.55} \tag{13}$$

where:

$$C = 90\mathrm{W}^{0.33}/(m^{0.66}\cdot\mathrm{K})$$

$$m = 0.12-0.2\log\{R_p\}_{\mu m}$$

Fig. 5 is the comparison of experiment result and Cooper's equation. In the calculation, the surface roughness $R_p$ is 0.3 μm as suggested by Refs. [27] for typical commercial tube. For R134a boiling outside smooth tube at the saturation temperature of 11 °C, deviations of experimental data and the equation were within −2.3% to 6.2%. The heat flux ranged from 10 to 50 kW/m$^2$.

The friction factors for smooth and enhanced tubes were also tested. As shown in Fig. 6, the friction factor data for the turbulent flow of smooth tube were found to be in good agreement with Filonenko correlation [29]. The deviation of experimental results and the equation was within −6.4% to 14.6%. It was higher at lower Reynolds number, where the pressure drop was also very low. For the enhanced tube, the tube side was enhanced with internal integral grooves. The friction factors were 130–160% higher than those predicted by the Filonenko equation. Experimental heat transfer enhancement ratio determined by Wison plot was 3.22. The heat transfer enhancement ratio was larger than the increase of friction factor. For most of the enhancement techniques [20,21,30], the heat transfer enhancement ratio was less than the increment of friction faction factor. A substantial heat transfer enhancement was mostly accompanying an large increase in the friction factor. The water side enhancement technique of this enhanced tube was particularly effective in heat transfer augmentation [20].

### 5.2. Overall heat transfer coefficient

Fig. 7 presents the overall heat transfer coefficient of smooth and enhanced tubes versus water velocity in falling film evaporation and pool boiling. The saturation temperature was 11 °C, and heat flux was maintained invariant at 30 kW/m$^2$. Heat transfer coefficients could be increased 3-fold for the velocity from 0.8 to 3.5 m/s compared with smooth tube. For the tubes that have the different overall heat transfer coefficient, if the heat transfer coefficient in tube side was the same, the difference was mostly caused by the variation of shell side heat transfer performance. It indicated that the heat transfer coefficient in pool boiling and falling film evaporation at this heat flux was similar for the enhanced tube in this study. At water velocity 2.2 m/s and heat flux 30 kW/m$^2$ in falling film evaporating, the ratio of thermal resistance for tube and shell side was 39.7% and 57.6% respectively. The shell side thermal resistance for the tube was larger than the tube side.

### 5.3. Shell side heat transfer coefficient

Fig. 8 shows the shell side falling film evaporation and pool boiling heat transfer coefficient of R134a at different heat flux. The experiments were conducted basically at the same condition. The saturation

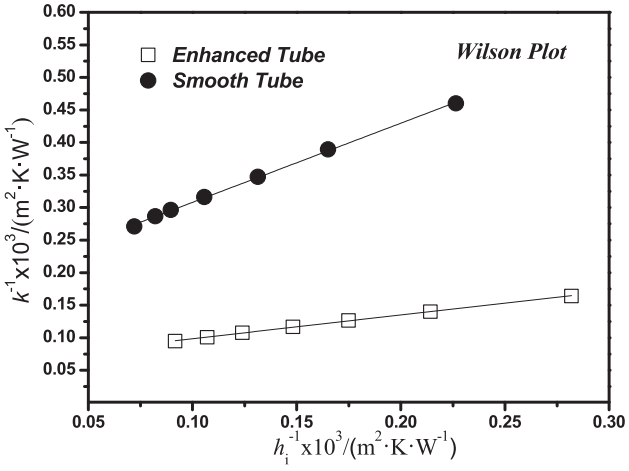


**Fig. 4.** Wilson plot of smooth and enhanced tubes.

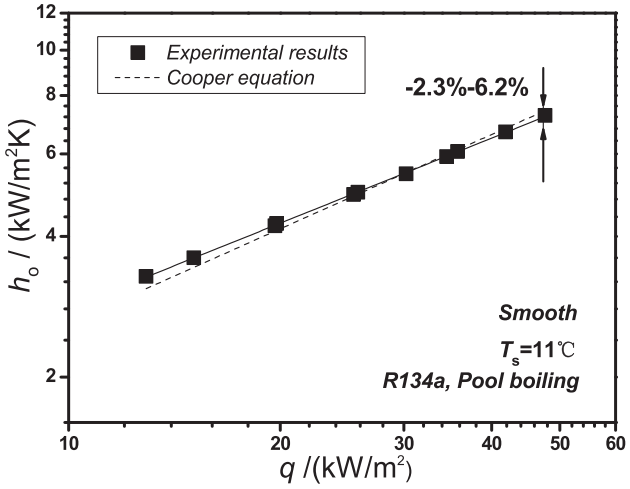


**Fig. 5.** Comparison of pool boiling heat transfer experiment results with Cooper's correlation.

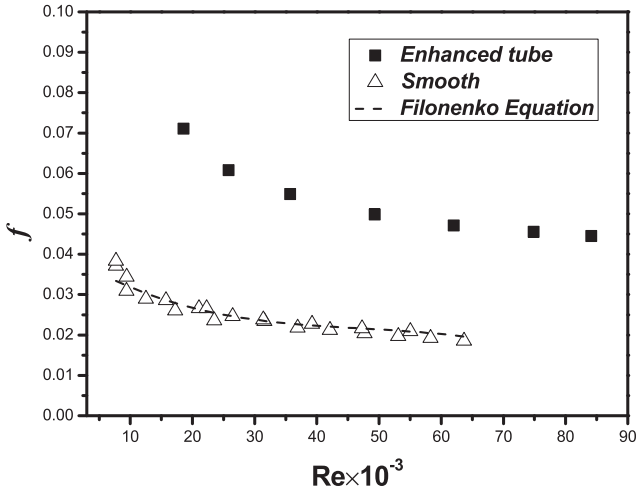


**Fig. 6.** Friction factor versus Reynolds number for smooth and enhanced tubes.

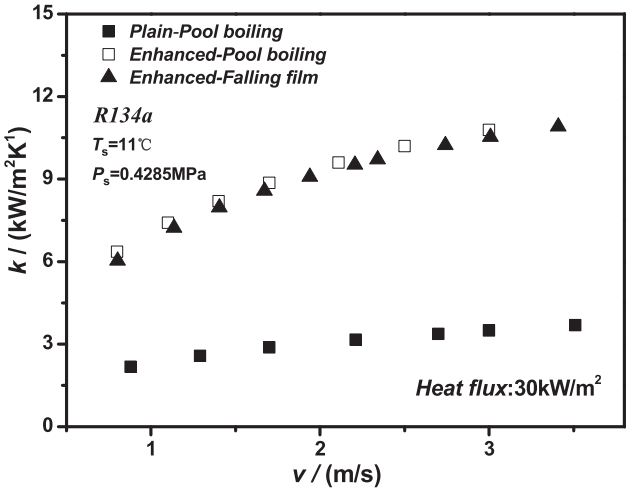


**Fig. 7.** Overall heat transfer coefficients versus water velocity in tube side at heat flux 30 kW/m$^2$.

temperature was 11 °C and saturate pressure was 0.4285 MPa. The water velocity in the tube side was 2.4 m/s and the uncertainty corresponding to the data reduction was essentially the same. The data for

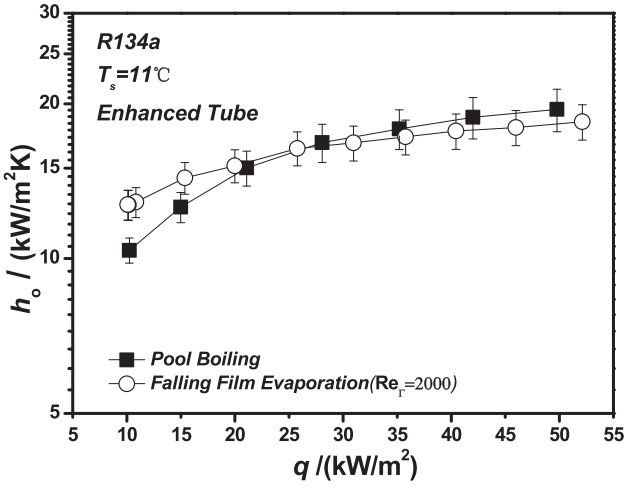


**Fig. 8.** Comparison of falling film and pool boiling heat transfer coefficients versus heat flux with the same enhanced tube.

the first row in the tube bundle were presented for comparison. The falling film Reynolds number was 2000 and heat flux was from 10 to 50 kW/m$^2$. During the falling film experiment, it was observed that the liquid film was evenly distributed outside the tubes. Most of the liquid film flowed downwards through the tube bundle and the splashing rate was rather small.

Heat transfer coefficients in pool boiling and falling film evaporation for the enhanced tube were increased by a factor of 2.1–4.9 compared with Cooper's equation (the uncertainties were accounted). The improvements in heat transfer coefficients might be attributed to the reentrant cavity structure. This enhanced tube was originally designed for pool boiling. As shown in Fig. 8, it had higher heat transfer coefficient at lower heat flux for falling film evaporation. The heat transfer coefficient at 10 kW/m$^2$ was 20% higher than pool boiling. While, the heat transfer coefficient for falling film was 2–5% lower at the heat flux more than 30 kW/m$^2$. The heat transfer coefficient increases as the increase of heat flux. While the heat transfer coefficient increasing rate for pool boiling was a little bit higher compared with falling film evaporation. Falling film evaporation were relatively effective at heat flux lower than 20 kW/m$^2$.

Figs. 9–13 show the falling film evaporation heat transfer coefficient versus falling film Reynolds number at a fixed heat flux. The general characteristics can be described as follows:

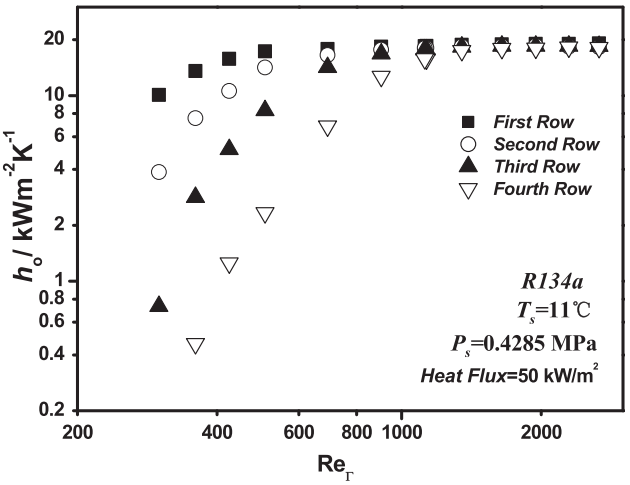


**Fig. 9.** Falling film heat transfer coefficients versus Re$_\Gamma$ at heat flux of 50 kW/m$^2$.

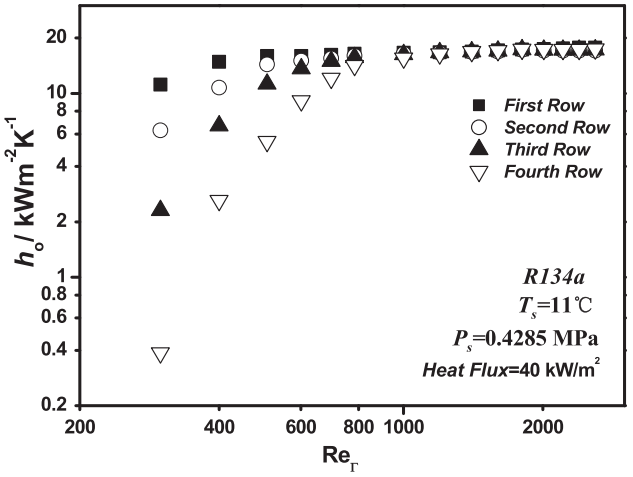


**Fig. 10.** Falling film heat transfer coefficients versus $Re_\Gamma$ at heat flux of 40 kW/m$^2$.

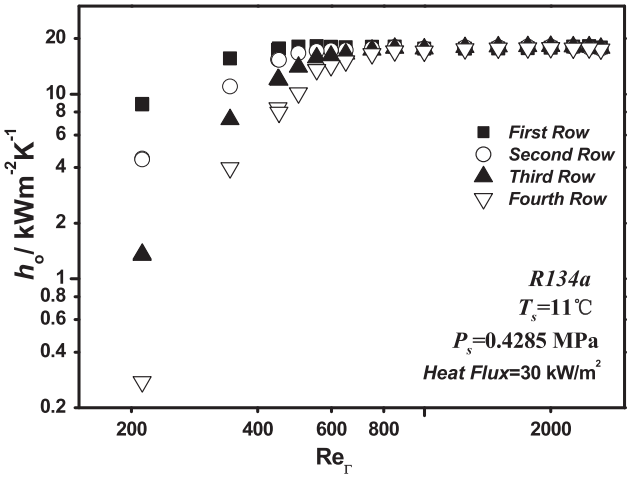


**Fig. 11.** Falling film heat transfer coefficients versus $Re_\Gamma$ at heat flux of 30 kW/m$^2$.

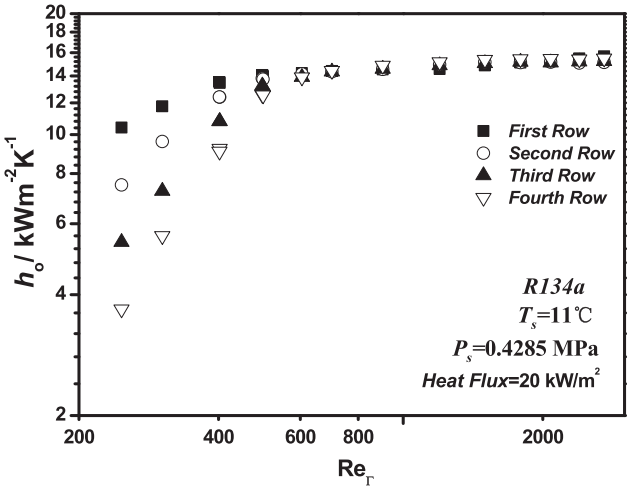


**Fig. 12.** Falling film heat transfer coefficients versus $Re_\Gamma$ at heat flux of 20 kW/m$^2$.

(1) The heat transfer performance was different for different tube rows. The first tube in the row typically had higher heat transfer coefficients. At the heat flux of 50 kW/m$^2$, the heat transfer coefficients of tubes were very close to each other at higher Reynolds number. When falling film Reynolds number was larger than 1000, it had a much less dependence on falling film heat transfer coefficient for different tube rows. The difference of falling film heat transfer coefficient was larger at lower film Reynolds number. As the evaporating rate was directly proportional to the liquid film thickness, the heat transfer coefficient was lower at lower tube bundles. For all the experimental cases, the bundle effect was obvious at lower film Reynolds number. A sudden drop off in the heat transfer coefficient was observed for all tubes with further decreasing of film flow rate. The decline in heat transfer performance was chiefly due to partial dry-out outside the tube surface. The significant drop-off Reynolds number was different for different heat flux. It was 1348 for the heat flux of 50 kW/m$^2$. This critical film Reynolds number was decreasing as the decrease of heat flux. It was 1000 for 40 kW/m$^2$, 850 for 30 kW/m$^2$, 600 for 20 kW/m$^2$, 450 for 10 kW/m$^2$.

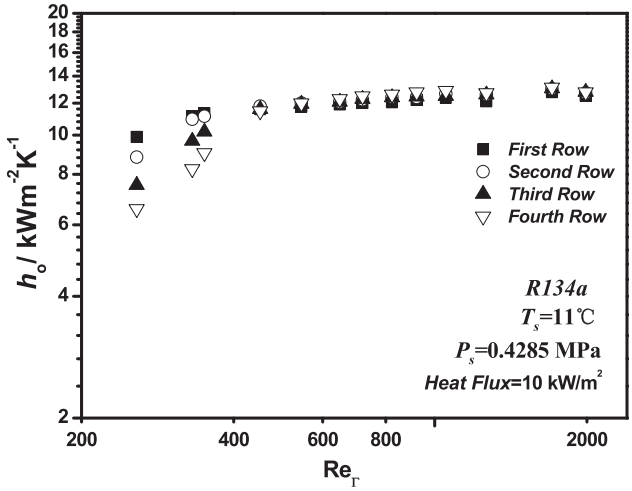


**Fig. 13.** Falling film heat transfer coefficients versus $Re_\Gamma$ at heat flux of 10 kW/m$^2$.

At lower heat flux 10 kW/m$^2$, the tubes in different vertical rows performed very similarly. The difference in heat transfer coefficient for the four tube rows was quite small at film Reynolds number from 300 to 2000. In this case, increment of falling film liquid flow rate had less effect to the efficiency of the chiller. The film-feed supply rate could be reduced at lower heat flux for a chiller.

(2) The transmission of energy in falling film evaporating was dominated by the phase change heat transfer. As the increment of film Reynolds number, an increase of only 10 percent of the falling film evaporation heat transfer coefficient was observed when the liquid film supply rate was sufficient. It indicated that the falling film evaporation heat transfer coefficient was weakly dependent on the forced convection heat transfer outside the tube surface. Evaporating heat transfer made the largest contribution to the overall falling film evaporating heat transfer coefficient. In the experiment, increase in the film flow rate as much as 5 times higher had rather minor effect on the falling film evaporating heat transfer coefficient when the liquid film overfeed rate was sufficient. For the Re from 500 to 2700 at heat flux of 20 kW/m$^2$, the increment of heat transfer coefficient was only 12% (partial dry-out conditions were excluded). It was becoming mild at higher heat flux. For the Re from 500 to 2700 at heat flux of 50 kW/m$^2$, the increment of heat transfer coefficient rate was only 9.8%.

### 5.4. Comparison of pool boiling and falling film heat transfer

It's commonly assumed that falling film heat transfer coefficient should be higher than pool boiling at the same experimental conditions, but it seems not accurate. As shown in Fig. 8 of present investigation, the falling film heat transfer coefficient was only higher at lower heat flux for the enhanced tube. The heat transfer coefficient in falling film evaporation showed less dependence on heat flux or tube wall superheat. At heat flux more than 20 kW/m$^2$, the heat transfer coefficient of falling film evaporation was even lower than pool boiling. Heat transfer coefficient was decreasing as the decrease of heat flux. From the heat flux 50–10 kW/m$^2$, falling film evaporation heat transfer coefficient decreased 30%.

Experimental results on the pool boiling and falling film heat transfer coefficient of smooth and enhanced tubes from the literature [5,6,9,10,28,31–36] were also compared in Figs. 14 and 15. The refrigerants included R134a, R114, R123, R245fa, and ammonia. The heat flux was investigated up to 160 kW/m$^2$ in the study of Zhao et al. [6].The diameters of tubes were in the range of 12.7–25.4 mm. The investigation on the falling film was mostly obtained with sufficient film-feed supply rate. The experimental data on both falling film evaporation and pool boiling for the same tube and same experimental conditions were both presented in the figures for comparison.

As shown in Fig. 14, the falling film evaporating heat transfer coefficient of smooth tubes with the diameter 12.7–25.4 mm were mostly higher than pool boiling at lower heat flux less than 40 kW/m$^2$. At the heat flux more than 60 kW/m$^2$, the heat transfer coefficients of falling film evaporation were mostly less than pool boiling. At higher heat flux more than 100 kW/m$^2$, the falling film evaporation heat transfer coefficient even decreased as the increment of heat flux. The dependence of falling film evaporation heat transfer coefficient on heat flux, exponent $n$ in the relationship of $h_o \propto q^n$ was less than pool boiling. It might be less than 0 for smooth tube in some cases. For the smooth tubes with refrigerant, the exponent is 0.67 with heat flux up to 250 kW/m$^2$ [28].

For the enhanced tubes as shown in Fig. 15, the dependence of heat transfer coefficient on the heat flux was also not apparent. The heat transfer coefficient of falling film evaporation was also higher than pool boiling at lower heat flux. For the reentrant cavity tubes in [5,9,10,33,34], the exponent of heat transfer coefficient versus heat flux was close or even less than 0. For Turbo-B5 tube in [9], the heat transfer coefficient of falling film evaporation and pool boiling was approaching at higher heat flux. For the other tubes in the investigations, the heat transfer coefficient was always higher than pool boiling. For the meshed tube in Refs. [35], the heat transfer coefficient of falling film and pool boiling were similar in the lower heat flux less than 20 kW/m$^2$. While at higher heat flux, the heat transfer coefficient in pool boiling was 20% higher than falling film evaporation.

For the falling film evaporation, the heat transfer was routinely supposed to be dominated by the densities of nucleation sites. Heat flux might be the leading factor like pool boiling and heat transfer should also be suction-evaporation mode [37]. Tube surface structure and the liquid distribution inside the tunnels determine how much the liquid being evaporated. For reentrant cavity tubes in the nucleate boiling region, increasing heat flux normally produces an increase in the population of nucleate sites. Heat flux 20 kW/m$^2$ seems to be the turning point for many enhanced tubes. When the heat flux was lower than 20 kW/m$^2$, the falling film evaporating heat transfer coefficient outside the same reentrant cavity tubes was mostly higher than pool boiling. When it was higher than 40 kW/m$^2$, the pool boiling heat transfer coefficient began to be even higher than falling film evaporation.

Despite numerous studies on falling film evaporation, some basic mechanisms for the heat transfer behavior still remain unclear. Nucleate boiling outside the tube is combined by the effects of flow rate, temperature, heat flux, distribution of liquid film, geometry, tube layout, and operating conditions. The behavior in the present study seems to be associated with the difference of bubble generation around the enhanced tubes. For the falling film evaporation, the bubbles outside the surface departed mostly by coalescence [38]. It grows slowly to a larger size. The bubble covered area is also getting larger and larger by continuous coalescence. Accumulated bubbles might flow away with the film flow. It will certainly separate the heating surface and liquid flow. However, the generated bubbles are pushed up by the static head of liquid pool in pool boiling. It detaches mainly by buoyancy. For the falling film evaporation, the pushing force is weak and bubbles are only driven by liquid flow. The boiling mode might be different for pool boiling and falling film evaporation, especially at higher heat flux. At lower heat flux, as the numbers of bubbles are less, the effect of bubble separating effect is negligible. While at rather higher heat flux and lower film flow rate, the effect is getting severe. As indicated above, at heat flux more than 100 kW/m$^2$, the heat transfer coefficient is even decreasing as the increment of heat flux for falling film evaporating; while it is 250 kW/m$^2$ for pool boiling. Pool boiling outside the enhanced surfaces performs slightly better than falling film evaporating at higher heat flux. If a sufficient liquid is provided within the closed cavity as pool boiling, the heat transfer rate should increase as pool boiling in the higher heat flux. Studies of pore size and distribution of bubbles for falling film evaporation might contribute to predications of the heat transfer coefficient.

## 6. Conclusions

In this paper, the falling film evaporation and pool boiling heat transfer coefficients of R134a outside one typical reentrant cavity tube were measured at different heat fluxes. The saturation temperature was 11 °C and the saturate pressure is 0.4285 MPa. The heat flux is maintained invariant from 10 to 50 kW/m$^2$. Falling film Reynolds number was from 200 to 2700. The internal water velocity was from 0.8 to 3.5 m/s. Based upon the test results and data from literature, the following conclusions can be drawn:

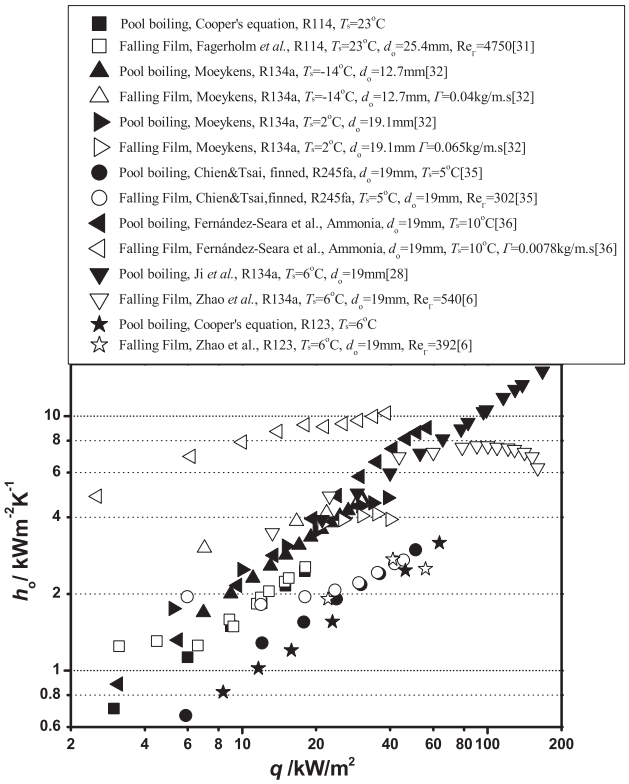


**Fig. 14.** Comparison of pool boiling and falling film heat transfer coefficients for smooth tubes from literature.

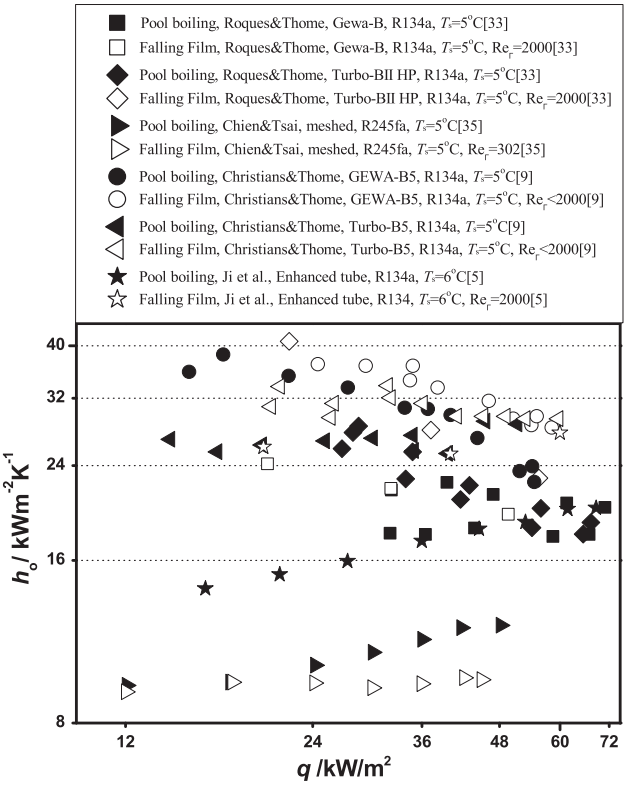


**Fig. 15.** Comparison of pool boiling and falling film heat transfer coefficients for enhanced tubes from literature.

(1) When the water side velocity increased from 0.8 to 3.5 m/s, the overall heat transfer coefficients in falling film evaporation increased 3-fold for the enhanced tube. Shell side falling film evaporation heat transfer coefficients was augmented by a factor of 2.5–4.
(2) The enhanced tube performed better in falling film evaporation than pool boiling at heat flux less than 30 kW/m$^2$, while it began to perform poorer than pool boiling at higher heat flux.
(3) For the same smooth and enhanced tubes in falling film evaporation, the dependence of heat transfer coefficient on the heat flux was different compared with pool boiling.
(4) Although the film and bubbles in falling film evaporating were pushed by the fluid flow, the transmission of energy was dominated by the phase change heat transfer.

## Acknowledgment

This work was supported by the National Key R&D Program of China (No. 2016YFB0601200) and National Natural Science Foundation of China (51776160).

## References

[1] J.R. Thome, Falling film evaporation: state-of-the-art review of recent work, J. Enhanc. Heat Transf. 6 (1999) 263–278.
[2] G. Ribatski, A.M. Jacobi, Falling-film evaporation on horizontal tubes – a critical review, Int. J. Refrig. 28 (2005) 635–653.
[3] A.M. Abed, M. Alghoul, M.H. Yazdi, A.N. Al-Shamani, K. Sopian, The role of enhancement techniques on heat and mass transfer characteristics of shell and tube spray evaporator: a detailed review, Appl. Therm. Eng. 75 (2015) 923–940.
[4] C.-Y. Zhao, W.-T. Ji, P.-H. Jin, W.-Q. Tao, Heat transfer correlation of the falling film evaporation on a single horizontal smooth tube, Appl. Therm. Eng. 103 (2016) 177–186.
[5] W.-T. Ji, C.-Y. Zhao, D.-C. Zhang, S. Yoshioka, Y.-L. He, W.-Q. Tao, Effect of vapor flow on the falling film evaporation of R134a outside a horizontal tube bundle, Int. J. Heat Mass Transf. 92 (2016) 1171–1181.
[6] C.-Y. Zhao, P.-H. Jin, W.-T. Ji, Y.-L. He, W.-Q. Tao, Experimental investigations of R134a and R123 falling film evaporation on enhanced horizontal tubes, Int. J. Refrig. 75 (2017) 190–203.
[7] X. Zeng, M.-C. Chyu, Z. Ayub, Experimental investigation on ammonia spray evaporator with triangular-pitch plain-tube bundle, Part I: tube bundle effect, Int. J. Heat Mass Transf. 44 (2001) 2299–2310.
[8] X. Zeng, M.-C. Chyu, Z. Ayub, Experimental investigation on ammonia spray evaporator with triangular-pitch plain-tube bundle, Part II: evaporator performance, Int. J. Heat Mass Transf. 44 (2001) 2081–2092.
[9] M. Christians, J.R. Thome, Falling film evaporation on enhanced tubes, part 1: experimental results for pool boiling, onset-of-dryout and falling film evaporation, Int. J. Refrig 35 (2012) 300–312.
[10] M. Christians, J.R. Thome, Falling film evaporation on enhanced tubes, part 2: prediction methods and visualization, Int. J. Refrig. 35 (2012) 313–324.
[11] E. Van Rooyen, J. Thome, Flow boiling data and prediction method for enhanced boiling tubes and tube bundles with R-134a and R-236fa including a comparison with falling film evaporation, Int. J. Refrig. 41 (2014) 60–71.
[12] C.-Y. Zhao, W.-T. Ji, P.-H. Jin, W.-Q. Tao, Cross vapor stream effect on falling film evaporation in horizontal tube bundle using R134a, Heat Transf. Eng. (2017).
[13] H.-W. Byun, D.H. Kim, S.H. Yoon, C.H. Song, K.H. Lee, O.J. Kim, Pool boiling performance of enhanced tubes on low gwp refrigerants, Appl. Therm. Eng. (2017).
[14] W.T. Ji, D.C. Zhang, N. Feng, J.F. Guo, M. Numata, G.N. Xi, W.Q. Tao, Nucleate pool boiling heat transfer of R134a and R134a-PVE lubricant mixtures on smooth and five enhanced tubes, J. Heat Transf. 132 (2010) 11502.
[15] W.-T. Ji, M. Numata, Y.-L. He, W.-Q. Tao, Nucleate pool boiling and filmwise condensation heat transfer of R134a on the same horizontal tubes, Int. J. Heat Mass Transf. 86 (2015) 744–754.
[16] A.R. Al-Badri, A. Bär, A. Gotterbarm, M.H. Rausch, A.P. Fröba, The influence of fin structure and fin density on the condensation heat transfer of R134a on single finned tubes and in tube bundles, Int. J. Heat Mass Transf. 100 (2016) 582–589.
[17] M. Habert, Falling Film Evaporation on a Tube Bundle with Plain and Enhanced Tubes, in: Ecocle Polytechnique Federale De Lausanne, 2009.
[18] V. Gnielinski, New equations for heat and mass transfer in turbulent pipe and channel flows, Int. J. Chem. Eng. 16 (1976) 359–368.
[19] W.T. Ji, D.C. Zhang, Y.L. He, W.Q. Tao, Prediction of fully developed turbulent heat transfer of internal helically ribbed tubes – an extension of Gnielinski equation, Int. J. Heat Mass Transf. 55 (2011) 1375–1384.
[20] W.-T. Ji, A.M. Jacobi, Y.-L. He, W.-Q. Tao, Summary and evaluation on single-phase heat transfer enhancement techniques of liquid laminar and turbulent pipe flow, Int. J. Heat Mass Transf. 88 (2015) 735–754.
[21] W.-T. Ji, A.M. Jacobi, Y.-L. He, W.-Q. Tao, Summary and evaluation on the heat transfer enhancement techniques of gas laminar and turbulent pipe flow, Int. J. Heat Mass Transf. 111 (2017) 467–483.
[22] J.W. Rose, Heat-transfer coefficients, Wilson plots and accuracy of thermal measurements, Exp. Therm. Fluid Sci. 28 (2004) 77–86.
[23] S.J. Kline, F.A. McClintock, Describing uncertainties in single-sample experiments, Mech. Eng. (1953) 3–8.
[24] R.J. Moffat, Describing the uncertainties in experimental results, Exp. Therm. Fluid Sci. (1988) 3–17.
[25] B. Cheng, W.Q. Tao, Experimental study of R-152a film condensation on single horizontal smooth tube and enhanced tubes, J. Heat Transf. 116 (1994) 266–270.
[26] W.-T. Ji, C.-Y. Zhao, D.-C. Zhang, Z.-Y. Li, Y.-L. He, W.-Q. Tao, Condensation of R134a outside single horizontal titanium, cupronickel (B10 and B30), stainless steel and copper tubes, Int. J. Heat Mass Transf. 77 (2014) 194–201.
[27] M.G. Cooper, Saturation nucleate pool boiling-a simple correlation, Int. Chem. Eng. Symp. Ser. 86 (1984) 785–792.
[28] W.-T. Ji, C.-Y. Zhao, Y.-L. He, W.-Q. Tao, Experimental validation of Cooper correlation at higher heat flux, Int. J. Heat Mass Transf. 90 (2015) 1241–1243.
[29] G.K. Filonenko, Hydraulic resistance in pipes, Teploenergetika 1 (1954) 40–44.
[30] J.F. Fan, W.K. Ding, J.F. Zhang, Y.L. He, W.Q. Tao, A performance evaluation plot of enhanced heat transfer techniques oriented for energy-saving, Int. J. Heat Mass Transf. 52 (2009) 33–44.
[31] N.-E. Fagerholm, A.-R. Ghazanfari, K. Kivioja, E. Järvinen, Boiling heat transfer performance of plain and porous tubes in falling film flow of refrigerant R114, Heat Mass Transf. 21 (1987) 343–353.
[32] S.A. Moeykens, Heat Transfer and Fluid Flow in Spray Evaporators with Application to Reducing Refrigerant Inventory, PHD Thesis Iowa State University, 1994, p. 560.
[33] J.-F. Roques, J. Thome, Falling films on arrays of horizontal tubes with R-134a, part I: boiling heat transfer results for four types of tubes, Heat Transfer Eng. 28 (2007) 398–414.
[34] J.-F. Roques, J. Thome, Falling films on arrays of horizontal tubes with R-134a, part II: flow visualization, onset of dryout, and heat transfer predictions, Heat Transfer Eng. 28 (2007) 415–434.
[35] L.-H. Chien, Y.-L. Tsai, An experimental study of pool boiling and falling film vaporization on horizontal tubes in R-245fa, Appl. Therm. Eng. 31 (2011) 4044–4054.
[36] J. Fernández-Seara, Á.A. Pardiñas, R. Diz, Experimental heat transfer coefficients of pool boiling and spray evaporation of ammonia on a horizontal plain tube, Int. J. Refrig. 67 (2016) 259–270.
[37] W. Nakayama, T. Daikoku, T. Nakajima, Effects of pore diameters and system pressure on saturated pool nucleate boiling heat transfer from porous surfaces, J. Heat Transf. 104 (1982) 286–291.
[38] G. Ribatski, J.R. Thome, A visual study of R134a falling film evaporation on enhanced and plain tubes, in: G. Liejin (Ed.), Proceedings of the 5th International Symposium on Multiphase Flow, Heat Mass Transfer and Energy Conversion, Xi'an Jiaotong University Press, Xi'an, China, 2005.